Published in final edited form as:
Magn Reson Med. 2007 January ; 57(1): 2–7. doi:10.1002/mrm.21134.

Compensation for Spin-Lock Artifacts Using an Off-Resonance Rotary Echo in $T_1\rho_{off}$-Weighted Imaging

Walter R.T. Witschey[1,*], **Arijitt Borthakur**[1,2], **Mark A. Elliott**[1,2], **Eric Mellon**[1,2], **Sampreet Niyogi**[2,3], **Chenyang Wang**[2,3], and **Ravinder Reddy**[1,2]

[1]Department of Biochemistry & Molecular Biophysics, University of Pennsylvania, Philadelphia, Pennsylvania, USA.

[2]Metabolic Magnetic Resonance Research and Computing Center, Department of Radiology, University of Pennsylvania, Philadelphia, Pennsylvania, USA.

[3]Department of Bioengineering, University of Pennsylvania, Philadelphia, Pennsylvania, USA.

Abstract

The origin of image artifacts in an off-resonance spin-locking experiment is shown to be imperfections in the excitation flip angle. A pulse sequence for off-resonance spin locking is implemented that compensates for imperfections in the excitation flip angle through an off-resonance rotary echo. The off-resonance rotary echo alternates the frequency offset and phase of the RF transmitter during two spin-locking pulses of equal duration. The underlying theory is detailed, and MR images demonstrate the effectiveness of the technique in agarose gel phantoms and in in vivo human brain at 3T.

Keywords

off-resonance $T_1\rho$; spin locking; $T_1\rho$-weighted imaging; rotary echo; $T_1\rho$ relaxation

The different magnetic relaxation properties of tissues make magnetic resonance imaging (MRI) one of the most clinically useful imaging modalities. Relaxation-dependent contrast is inherent to conventional T_1- and T_2-weighted images as well as the more recent steady-state free precession (SSFP) T_1/T_2-weighted images. Since relaxation times vary among healthy and diseased tissues, these techniques can be used to distinguish the diseased tissues in MR images. In addition to the widely employed T_1 and T_2 relaxation contrast techniques, a small but increasing number of studies are devoted to examining $T_1\rho$ relaxation contrast, in which tissue magnetization is “locked” by an on-resonance RF field. Redfield (1) showed that the $T_1\rho$ relaxation time characterizes the spin-lattice relaxation in the rotating frame. In most cases, as the amplitude of the locking RF field approaches zero, $T_1\rho$- weighted imaging is functionally equivalent to T_2- weighted imaging, since both generate tissue contrast based on the disappearance of transverse magnetization.

In practice, $T_1\rho$-weighted imaging offers several advantages over T_1- and T_2-weighted imaging. For example, $T_1\rho$-weighted imaging is sensitive to the slow motional processes in the 0.5–3 kHz range, such as proton exchange with amides and hydroxyl groups in proteins and residual dipole–dipole interactions (2,3). To mention a few applications, $T_1\rho$-weighted

*Correspondence to: Walter Witschey, B.S., Department of Biochemistry and Molecular Biophysics, University of Pennsylvania, B1 Stellar-Chance Laboratories, 422 Curie Boulevard, Philadelphia, PA 19104-6100. witschey@med.upenn.edu.

imaging has shown improved contrast between healthy brain or breast tissues and tumors in mice (4) and humans (5,6), tracked the degeneration of the patellar cartilage matrix (7,8), is sensitive to posttraumatic cartilage injury (9) and has shown sensitivity to degradation of the nucleus pulposus in studies of degenerative intervertebral disc disease (10,11) and enabled the indirect detection of metabolic $H_2^{17}O$ in vivo (12,13). This approach presents some difficulties compared to traditional relaxation contrast techniques, however. Long-duration RF pulses may cause coil damage, the specific absorption rate (SAR) delivered to tissues during a $T_1\rho$ sequence is high, and both B_0 and B_1 imperfections are significant sources of artifacts.

To overcome three of these difficulties (coil damage, high SAR, and B_1 imperfections), we developed a $T_1\rho_{off}$ pulse sequence that implements an off-resonance "rotary echo" during spin locking. An off-resonance spin lock reduces the spin-lock RF field strength ω_1 by increasing the off-resonance component $\Delta\omega_0$ to achieve the same effective field strength, and thus reduces the SAR and ω_1 power demands on the RF coil. A rotary echo reduces artifacts due to B_1 inhomogeneity. $T_1\rho_{off}$ is an intrinsically different relaxation time from $T_1\rho$, and instead combines both $T_1\rho$- and T_1-type contrast. In particular, when an off-resonance RF pulse is delivered far from resonance ($\Delta\omega_0 \gg \omega_1$), $T_1\rho_{off}$ approaches T_1 and on-resonance $T_1\rho_{off}$ becomes $T_1\rho$. Here we generalize the rotary echo to the off-resonance case using product operator theory and show that it reduces imperfect B_1 MR image artifacts during off-resonance spin locking. In previous studies, off-resonance spin locking showed sensitivity to acute rat cerebral ischemia for $\Delta\omega_{RF} < 2.5$ kHz (14), and was used to obtain single-shot measurements of $T_1\rho_{off}$ in the human breast (15). Despite the decrease in sensitivity to tissue pathology that occurs with decreasing $\omega_1/\omega\Delta_{RF}$ (16), off-resonance spin locking may be useful for situations in which $\Delta\omega_0$ inhomogeneity artifacts prohibit an on-resonance spin lock, particularly at higher B_0 field strengths.

The geometry of the system during an off-resonance spin lock in the rotating frame is shown in Fig. 1. Magnetization is flipped parallel to the effective field, such that the flip angle $\alpha = \phi$, where the effective field ω_{eff} makes an angle with the z-axis:

$$\varphi=\tan^{-1}\left(\frac{\omega_1}{\Delta\omega}\right). \quad [1]$$

In the on-resonance case, $\omega_{eff} = \omega_1$ and $\phi = 90°$.

Solomon (17) first introduced the rotary echo to correct for imperfections in the RF field. On-resonance, spins accumulate a phase $\omega_1\tau$ because of nutation due to the RF field. In particular, an inhomogeneous B_1 field will cause the spin phase to vary throughout the sample and cause a decay of the net magnetization throughout the sample. Solomon (17) realized that if a second B_1 pulse that is 180° out of phase with the first is applied for the same duration, the spins will accumulate the exact opposite phase $\omega_1\tau$ and an echo will be formed at 2τ. Sears (18,19) extended the rotary echo to off-resonance spins to remove the dipolar broadening in solid $CFCl_3$. Further, Rhim et al. (20) used an off-resonance rotary echo to compensate for inhomogeneity in the RF field in time reversal experiments on dipolar coupled spins. Notably, the current implementation is used not only to compensate for the loss of coherence during the RF pulse, but also to correct for nutations about the effective field as a result of an imperfect excitation. Indeed, as we will show in Eq. [13], the origin of spin-lock artifacts is nutation about the effective field rather than the loss of phase coherence, which may shorten only the apparent relaxation time during the applied RF pulse.

More recently, several $T_1\rho$-weighted pulse sequences with artifact correction have been implemented in MRI (see Table 1). Charagundla et al. (21) eliminated artifacts from both B_1

imperfections and flip angles $\alpha \neq 90°$ (usually also the result of an imperfect B_1) in $T_1\rho$-weighted imaging. By reducing these artifacts, it became possible to measure the spatial distribution of $T_1\rho$ relaxation times accurately (22). A complementary technique uses adiabatic excitation to correct for an imperfect flip angle (16). We suggest that an off-resonance rotary echo is useful for spin-locking off-resonance, corrects for both B_1 imperfections and flip angles $\alpha \neq \phi$, and can also complement an adiabatic excitation.

A traditional off-resonance, $T_1\rho_{off}$-weighted imaging sequence is shown in Fig. 2 (sequence 1). Magnetization is $T_1\rho_{off}$-weighted during the spin-locking cluster and spatially encoded in two or three dimensions by a spin-echo imaging sequence. If the flip angle $\alpha \neq \phi$, images will have banding artifacts, as shown in Fig. 3.

THEORY

The origin of the banding artifacts can be shown with the use of product operator theory. Although the on-resonance spin-lock theory of the rotary echo is well described by quantum mechanical (20) or Bloch (21) treatments, the off-resonance case has not been examined. Following the notation of Levitt (23), the density matrix at equilibrium is given by

$$\rho(0^-)=\mathrm{I_Z}, \qquad [2]$$

where we omit the unity operator 1 and the Boltzmann factor for compactness. Ideally, a uniform pulse of flip angle $\alpha = \phi$ nutates the magnetization parallel to the effective magnetic field ω_{eff} so that immediately after the pulse

$$\rho(0^+)=\mathrm{R_X}(-\varphi)\mathrm{I_Z}\mathrm{R_X}(\varphi), \qquad [3]$$

where the pulse nutation is assumed to be instantaneous, and thus $\mathrm{R_X}(-\varphi) = e^{-i\varphi I_X}$. The density matrix evolves under the influence of the effective field ω_{eff}, so

$$\rho(\tau^-)=\mathrm{R_{Z'}}(\omega_{eff}\tau)\mathrm{R_X}(-\varphi)\mathrm{I_Z}\mathrm{R_X}(\varphi)\mathrm{R_{Z'}}\cdot(-\omega_{eff}\tau), \qquad [4]$$

where the effective field in the rotating frame is $\omega_{eff}=\sqrt{\omega_1^2+\Delta\omega^2}$, the evolution propagator is $\mathrm{R_{Z'}}(\omega_{eff}\tau) = e^{-i\omega_{eff} I_{Z'}\tau}$ and z' denotes the axis of the effective field. After $T_1\rho_{off}$-weighting, the magnetization is stored along the z-axis with a $-\phi$ pulse:

$$\rho(\tau^+)=\mathrm{R_X}(\varphi)\mathrm{R_{Z'}}(\omega_{eff}\tau)\mathrm{R_X}(-\varphi)\mathrm{I_Z}\mathrm{R_X}(\varphi)\mathrm{R_{Z'}}(-\omega_{eff}\tau)\mathrm{R_X}(-\varphi). \qquad [5]$$

To examine the density matrix evolution during the spin-locking pulse, we transform the density matrix to the tilted rotating frame using

$$\mathrm{R_{Z'}}(\omega_{eff}\tau)=\mathrm{R_X}(-\varphi)\mathrm{R_Z}(\omega_{eff}\tau)\mathrm{R_X}(\varphi). \qquad [6]$$

Combining Eqs. [5] and [6] yields

$$\rho(\tau^+)=\mathrm{R_X}(\varphi)\mathrm{R_X}(-\varphi)\mathrm{R_Z}(\omega_{eff}\tau)\mathrm{R_X}(\varphi)\mathrm{R_X}(-\varphi)\mathrm{I_Z}\mathrm{R(inv)}, \qquad [7]$$

where R(inv) denotes the inverse operators applied to the right of the density matrix at $\rho(0^-)$. Now, $R_X(\varphi)R_X(\varphi) = 1$. Since at $\tau = 0^-$ the density matrix is proportional to I_Z, the commutator $[R_Z(\omega_{eff}\tau), I_Z] = 0$. Consequently, the density matrix in Eq. [7] is reduced to

$$\rho(\tau^+)=\rho(0^-), \quad [8]$$

in addition to the usual $T_{1\rho off}$ relaxation.

As Soloman (17) showed empirically, Eq. [8] is not correct in the presence of an imperfect B_1 field, but can be corrected with a rotary echo. In addition, as the result of an imperfect spin flip where $\alpha \neq \phi$, the magnetization now makes a small angle $\Delta\varphi$ to ω_{eff}:

$$\rho(0^+)=\mathrm{R_x}(-\varphi+\Delta\varphi)\mathrm{I_z}\mathrm{R_x}(\varphi-\Delta\varphi). \quad [9]$$

Since the magnetization is no longer parallel to ω_{eff}, Eq. [7] no longer simply reproduces $\rho(\tau^+) = \rho(0^-)$ in Eq. [8]. As a result, ω_{eff} modulates the density matrix by $R_Z(\omega_{eff}\tau)$, and signal oscillations proportional to both ω_{eff} and τ are observed. Figure 3 shows the artifacts produced because of this oscillation.

Suppose now that ω_1 is broken into two pulses of equal duration, as shown in Fig. 2 (sequence 2). During the first period $\tau/2$ (Fig. 2a), ω_{eff} modulates the density operator as in Eq. [6]. During the second period $\tau/2$ (Fig. 2b), the phase of ω_{eff} is rotated 180°. The transformation to the tilted rotating frame during this period may be written as

$$\mathrm{R_{z'}}(\omega_{\mathrm{eff}}\tau/2)=\mathrm{R_x}(\pi)\mathrm{R_x}(-\varphi)\mathrm{R_z}(\omega_{\mathrm{eff}}\tau/2)\mathrm{R_x}(\varphi)\mathrm{R_x}(-\pi). \quad [10]$$

Since $[R_X(\pi), R_X(-\varphi)] = 0$, the π rotation inverts the direction of nutation:

$$\mathrm{R_{z'}}(\omega_{\mathrm{eff}}\tau/2)=\mathrm{R_x}(-\varphi)\mathrm{R_z}(-\omega_{\mathrm{eff}}\tau/2)\mathrm{R_x}(\varphi). \quad [11]$$

As before, the density matrix at time $\tau/2$ is

$$\rho(\tau/2)=\mathrm{R_{z'}}(\omega_{\mathrm{eff}}\tau/2)\mathrm{R_x}(-\varphi+\Delta\varphi)\mathrm{I_z}\mathrm{R_x}(\varphi-\Delta\varphi)\mathrm{R_{z'}}(-\omega_{\mathrm{eff}}\tau/2). \quad [12]$$

The density matrix now evolves according to Eq. [11], so

$$\rho(\tau^-)=\mathrm{R_x}(-\varphi)\mathrm{R_z}(-\omega_{\mathrm{eff}}\tau/2)\mathrm{R_x}(\varphi)\mathrm{R_x}(-\varphi)\times R_z(\omega_{\mathrm{eff}}\tau/2)R_x(\varphi)R_x(-\varphi+\Delta\varphi)\mathrm{I_z}\mathrm{R(inv)}. \quad [13]$$

Finally, Eq. [13] reduces to

$$\rho(\tau^-)=\mathrm{R_x}(-\varphi+\Delta\varphi)\mathrm{I_z}\mathrm{R_x}(\varphi-\Delta\varphi). \quad [14]$$

The effects of the nutation $R_Z(\omega_{eff}\tau)$ in Eq. [13] are completely eliminated in Eq. [14] by $R_X(\pi)$. Of course, the form of $R_X(\pi)$ in Eq. [10] depends on whether spin locking is performed on-resonance ($\omega_{eff} = \omega_1$) or off-resonance ($\omega_{eff} \neq \omega_1$). We examine both of these cases below.

RESULTS

Phase inversion of ω_1 (±180°) meets the condition of $R_X(\pi)$ in Eq. [10] on-resonance, and is shown in Fig. 3 to reduce artifacts in 3% agarose phantoms. For example, if ω_1 is parallel to the *y*-axis during the first spin-locking period, then ω_1 must be parallel to the −*y*-axis during the second spin-locking period. Physically, when the flip angle $\alpha \neq \phi$, the magnetization makes an angle $\Delta\phi$ with the *xy*-plane. During the first spin-locking period, magnetization nutates about the spin-locking axis *y* for a time $\tau/2$. In the second spin-locking period, the sense of precession is reversed ($\omega_1 \rightarrow -\omega_1$) and the magnetization returns to its orientation prior to spin locking.

Combined inversion of ω_1 and inversion of $\Delta\omega$, the transmitter offset frequency, satisfies $R_X(\pi)$ in Eq. [10] and is shown experimentally in Fig. 3. Once again, if $\alpha \neq \phi$, the magnetization makes an angle $\Delta\phi$ with ω_{eff}. During the first spin-locking period, magnetization nutates about ω_{eff}. Without inversion of the ω_{eff}, the signal oscillates. If during the second spin-locking period, $\omega_1 \rightarrow -\omega_1$ and $\Delta\omega \rightarrow -\Delta\omega$, the axis of ω_{eff} will be inverted and the sense of precession about ω_{eff} will be reversed. This condition is called phase and frequency inversion.

The pulse sequence used to reduce off-resonance spin-locking artifacts is shown in Fig. 2, sequence 2, and is contrasted with the conventional off-resonance spin lock shown in Fig. 2, sequence 1. Magnetization is excited along the direction of the effective field with a hard pulse $R_X(-\varphi)$, where it is spin-locked by two phase and frequency symmetric spin-locking pulses (+*y*, +$\Delta\omega$ and −*y*, −$\Delta\omega$). Consequently, the magnetization is stored along the *z*-axis with another hard pulse. During spin locking, the magnetization nutates first around the effective field (Fig. 2a) and is refocused during the second $\tau/2$ period by nutation in the opposite direction (Fig. 2b).

DISCUSSION

While it may be useful for single-spin systems, the off-resonance rotary echo has limited applicability to NMR spectroscopy because it cannot simultaneously rephase spins precessing at different frequencies. For example, suppose two spins are spin-locked off-resonance, where the frequencies of the two precessing spins are $\Delta\omega_1$ and $\Delta\omega_2$ in the rotating frame. Frequency inversion of the first spin ($\Delta\omega_1 \rightarrow -\Delta\omega_1$) cannot simultaneously bring the second spin back into phase with the first at the end of the spin-locking sequence ($t = \tau$). Despite this limitation, the off-resonance rotary echo pulse sequence in Fig. 2, sequence 2, is still useful for MRI because most imaging systems have a single resonant frequency. An additional complication is the presence of any appreciable B_0 inhomogeneity, which may cause local spin density to precess off-resonance; however, the condition for an effective off-resonance spin lock $\omega_{eff}=\sqrt{\omega_1^2+\Delta\omega_{RF}^2} \gg \Delta\omega_0$ is in fact an easier requirement to fulfill compared to the on-resonance condition $\omega_1 \gg \Delta\omega_0$. We demonstrate the utility of the off-resonance spin lock for imaging the human brain at 3T in Fig. 4 and call attention to the severe deviation of the initial excitation flip angle (α = 65°) from the nominal flip angle (α = 45°) for $\omega_1 = \Delta\omega_{RF}$ = 400 Hz. For this reason, surface coil $T_{1\rho_{off}}$-weighted imaging in particular benefits from the compensated rotary echo.

It is possible to estimate the reduction in SAR during the off-resonance spin lock using a model for SAR deposited in the human head by a quadrature birdcage coil developed by Collins et al. (24). It was shown that

$$SAR(\alpha,\tau)=f\left(\frac{3ms}{\tau}\right)^2\left(\frac{\alpha}{90^\circ}\right)^2 SAR_{90,3ms}, \qquad [15]$$

where the SAR is a function of the shape factor f(= 1 for a rectangular pulse), flip angle α, pulse duration τ, and coefficient $SAR_{90°,3\ ms}$ = 1.46 W/kg for a 3-ms, 90° rectangular pulse at 1.5T. Considering a single 500 Hz spin-locking pulse delivered for 100 ms, the average SAR delivered with TR = 3 s is approximately 2 W/kg, which is well under the 8 W/kg FDA mandated restriction in the head. For pulse sequences with shorter TR, such as a $T_1\rho$-weighted 3D gradient-echo (GRE) or $T_1\rho$-weighted balanced-SSFP sequence, the average SAR can often surpass FDA limitations. For example, the average SAR delivered during a $T_1\rho$-weighted 3D GRE sequence with TR = 300 ms is nearly 18 W/kg, but can be reduced to less than 8 W/kg by implementing a $T_1\rho_{off}$ sequence with ω_{eff} = 500 Hz, ω_1 = 325 Hz and $\Delta\omega_0$ = 380 Hz. Even if assumptions about the filling factor or $SAR_{90,3ms}$ are incorrect, Eq. [15] predicts that the reduction in SAR will be $(B_{1,off}/B_{1,on})^2$ and the SAR will be reduced to a fraction of that obtained in an on-resonance $T_1\rho$-weighted experiment. In addition, one can reduce the total scan time by lowering the minimum TR necessary to maintain FDA guidelines.

One unusual consequence may emerge from samples with an asymmetric *z*-spectrum, where the magnetization transfer (MT) effect may vary between the two spin-locking pulses. For example, suppose an off-resonance spin-locking or saturation experiment is performed in the presence of an asymmetric *z*-spectrum. The signal intensity might be expected to vary with the spin-locking length and the asymmetry in the *z*-spectrum. Also, in the conventional off-resonance spin lock, as $\tau \rightarrow \infty$ the magnetization approaches a steady state M_{eff} along the direction of the effective field ω_{eff}. During a rotary echo, M_{eff} is expected to change halfway through the spin lock and consequently change the resultant image contrast. There are no obvious differences in contrast for τ < 100 ms, although they certainly may exist. $\Delta\omega_{RF}$ inversion may even null tissue magnetization if it is timed appropriately.

CONCLUSIONS

We have introduced a spin-locking sequence that reduces B_1 artifacts by means of a frequency- and phase-inverted spin-locking pulse cluster. In agreement with theory, we demonstrated that B_1 nutation can be reversed by a 180° inversion of the effective field on- or off-resonance, and showed that B_1 artifacts were reduced in experiments on agarose phantoms. We expect that this off-resonance rotary echo will be useful for off-resonance spin locking, since the technique removes complicating image artifacts and preserves exponential $T_1\rho_{off}$ decay of the signal while it reduces the required spin-locking RF amplitude.

Acknowledgments

The authors thank Luke Bloy, Jeremy Wellen, and Susanta Sarkar for stimulating discussions and technical expertise. This study was performed at the Metabolic Magnetic Resonance Research and Computing Center, an NIH-supported resource center (NIH RR02305).

Grant sponsor: National Institutes of Health (NIH); Grant numbers: R01AR045404; R01AR051041.

REFERENCES

1. Redfield AG. Nuclear magnetic resonance saturation and rotary saturation in solids. Phys Rev 1955;98:1787–1809.
2. Duvvuri U, Goldberg AD, Kranz JK, Hoang L, Reddy R, Wehrli FW, Wand AJ, Englander SW, Leigh JS. Water magnetic relaxation dispersion in biological systems: the contribution of proton exchange and implications for the noninvasive detection of cartilage degradation. Proc Natl Acad Sci USA 2001;98:12479–12484. [PubMed: 11606754]
3. Akella SV, Regatte RR, Wheaton AJ, Borthakur A, Reddy R. Reduction of residual dipolar interaction in cartilage by spin-lock technique. Magn Reson Med 2004;52:1103–1109. [PubMed: 15508163]

4. Poptani H, Duvvuri U, Miller CG, Mancuso A, Charagundla S, Fraser NW, Glickson JD, Leigh JS, Reddy R. T1rho imaging of murine brain tumors at 4 T. Acad Radiol 2001;8:42–47. [PubMed: 11201456]
5. Aronen HJ, Ramadan UA, Peltonen TK, Markkola AT, Tanttu JI, Jaaskelainen J, Hakkinen AM, Sepponen R. 3D spin-lock imaging of human gliomas. Magn Reson Imaging 1999;17:1001–1010. [PubMed: 10463651]
6. Santyr GE, Henkelman RM, Bronskill MJ. Spin locking for magnetic resonance imaging with application to human breast. Magn Reson Med 1989;12:25–37. [PubMed: 2607958]
7. Wheaton AJ, Casey FL, Gougoutas AJ, Dodge GR, Borthakur A, Lonner JH, Schumacher HR, Reddy R. Correlation of T1rho with fixed charge density in cartilage. J Magn Reson Imaging 2004;20:519–525. [PubMed: 15332262]
8. Wheaton AJ, Dodge GR, Borthakur A, Kneeland JB, Schumacher HR, Reddy R. Detection of changes in articular cartilage proteoglycan by T(1rho) magnetic resonance imaging. J Orthop Res 2005;23:102–108. [PubMed: 15607881]
9. Lozano J, Li X, Link TM, Safran M, Majumdar S, Ma CB. Detection of posttraumatic cartilage injury using quantitative T1rho magnetic resonance imaging. A report of two cases with arthroscopic findings. J Bone Joint Surg Am 2006;88:1349–1352. [PubMed: 16757771]
10. Johannessen W, Auerbach JD, Wheaton AJ, Kurji A, Borthakur A, Reddy R, Elliott DM. Assessment of human disc degeneration and proteoglycan content using T1rho-weighted magnetic resonance imaging. Spine 2006;31:1253–1257. [PubMed: 16688040]
11. Auerbach JD, Johannessen W, Borthakur A, Wheaton AJ, Dolinskas CA, Balderston RA, Reddy R, Elliott DM. In vivo quantification of human lumbar disc degeneration using T(1rho)-weighted magnetic resonance imaging. Eur Spine J 2006;15:S338–S344. [PubMed: 16552534]
12. Tailor DR, Poptani H, Glickson JD, Leigh JS, Reddy R. High-resolution assessment of blood flow in murine RIF-1 tumors by monitoring uptake of H217O with proton T1rho-weighted imaging. Magn Reson Med 2003;49:1–6. [PubMed: 12509813]
13. Tailor DR, Roy A, Regatte RR, Charagundla SR, McLaughlin AC, Leigh JS, Reddy R. Indirect 17O-magnetic resonance imaging of cerebral blood flow in the rat. Magn Reson Med 2003;49:479–487. [PubMed: 12594750]
14. Grohn OH, Makela HI, Lukkarinen JA, DelaBarre L, Lin J, Garwood M, Kauppinen RA. On- and off-resonance T1rho MRI in acute cerebral ischemia of the rat. Magn Reson Med 2003;49:172–176. [PubMed: 12509834]
15. Fairbanks EJ, Santyr GE, Sorenson JA. One-shot measurement of spin-lattice relaxation-times in the off-resonance rotating-frame using MR-imaging, with application to breast. J Magn Reson Ser B 1995;106:279–283. [PubMed: 7719626]
16. Santyr GE, Fairbanks EJ, Kelcz F, Sorenson JA. Off-resonance spin locking for MR imaging. Magn Reson Med 1994;32:43–51. [PubMed: 8084236]
17. Soloman I. Rotary spin echoes. Phys Rev Lett 1959;2:301–302.
18. Sears REJ. Off-resonance rotary spin echoes in dipolar broadened solids. Bull Am Phys Soc 1970;15:275.
19. Sears REJ. F-19 anistropic chemical-shift in solid CFCL3. Bull Am Phys Soc 1972;17:573.
20. Rhim WK, Pines A, Waugh JS. Time-reversal experiments in dipolar-coupled spin systems. Phys Rev B 1971;3:684–696.
21. Charagundla SR, Borthakur A, Leigh JS, Reddy R. Artifacts in T1ρ- weighted imaging: correction with a self-compensating spin-locking pulse. J Magn Reson 2003;162:113–121. [PubMed: 12762988]
22. Regatte RR, Akella SV, Borthakur A, Kneeland JB, Reddy R. In vivo proton MR three-dimensional T1rho mapping of human articular cartilage: initial experience. Radiology 2003;229:269–274. [PubMed: 14519880]
23. Levitt, MH. Spin dynamics: basics of nuclear magnetic resonance. New York: John Wiley & Sons, Ltd.; 2001.
24. Collins CM, Li S, Smith MB. SAR and B_1 field distributions in a heterogeneous human head model within a birdcage coil. Magn Reson Med 1998;40:847–856. [PubMed: 9840829]

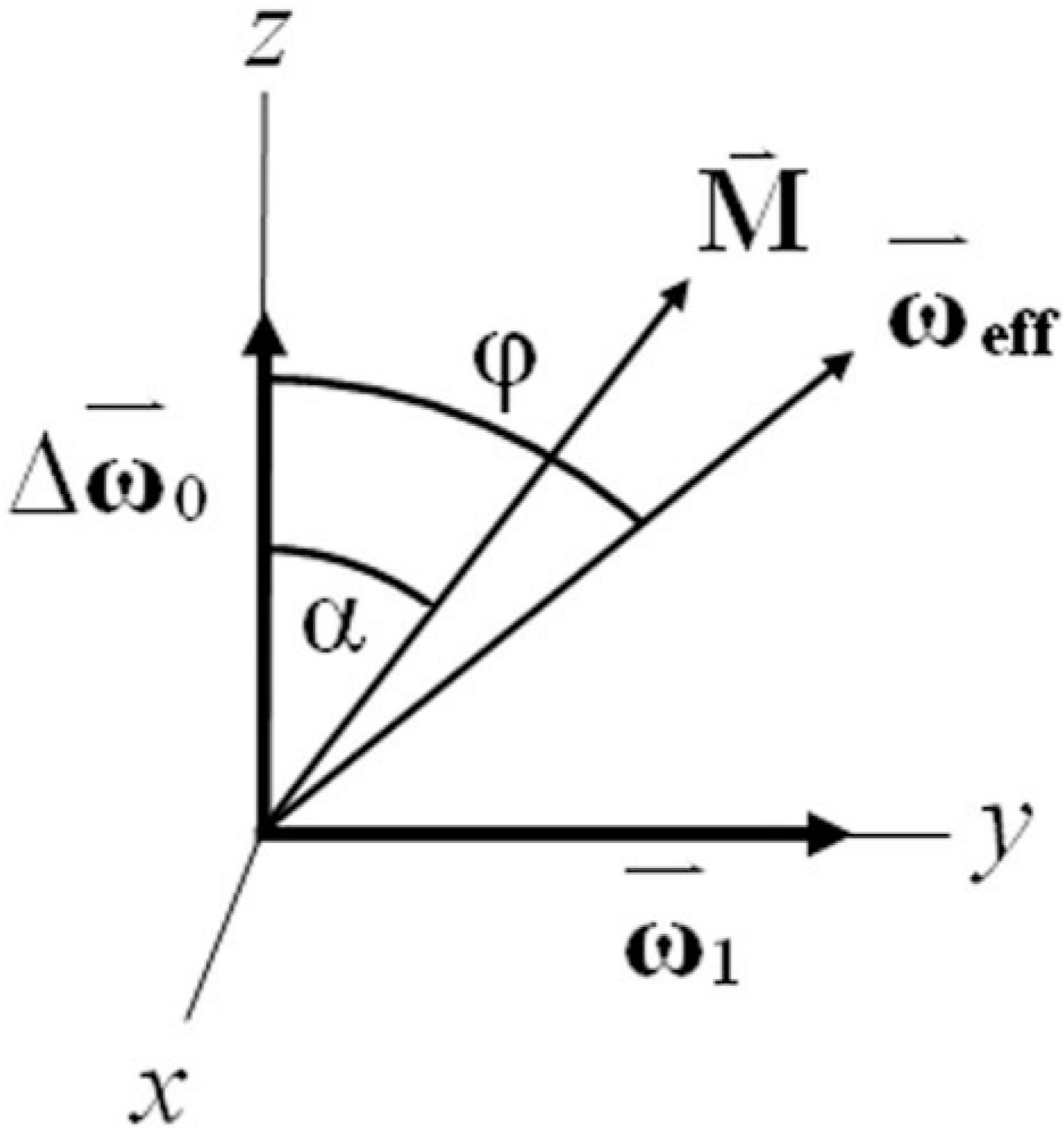

FIG. 1.

Off-resonance spin-locking geometry. The effective field ω_{eff} makes an angle $\varphi = \tan^{-1}(\omega_1/\Delta\omega)$ with the *z*-axis. To perform off-resonance spin locking, the magnetization must be flipped parallel to the effective field such that the flip angle $\alpha = \phi$; however, B_1 imperfections cause deviations in the expected flip angle $\alpha = \phi - \Delta\phi$. In on-resonance spin-locking experiments, $\omega_{eff} = \omega_1$ and $\phi = 90°$.

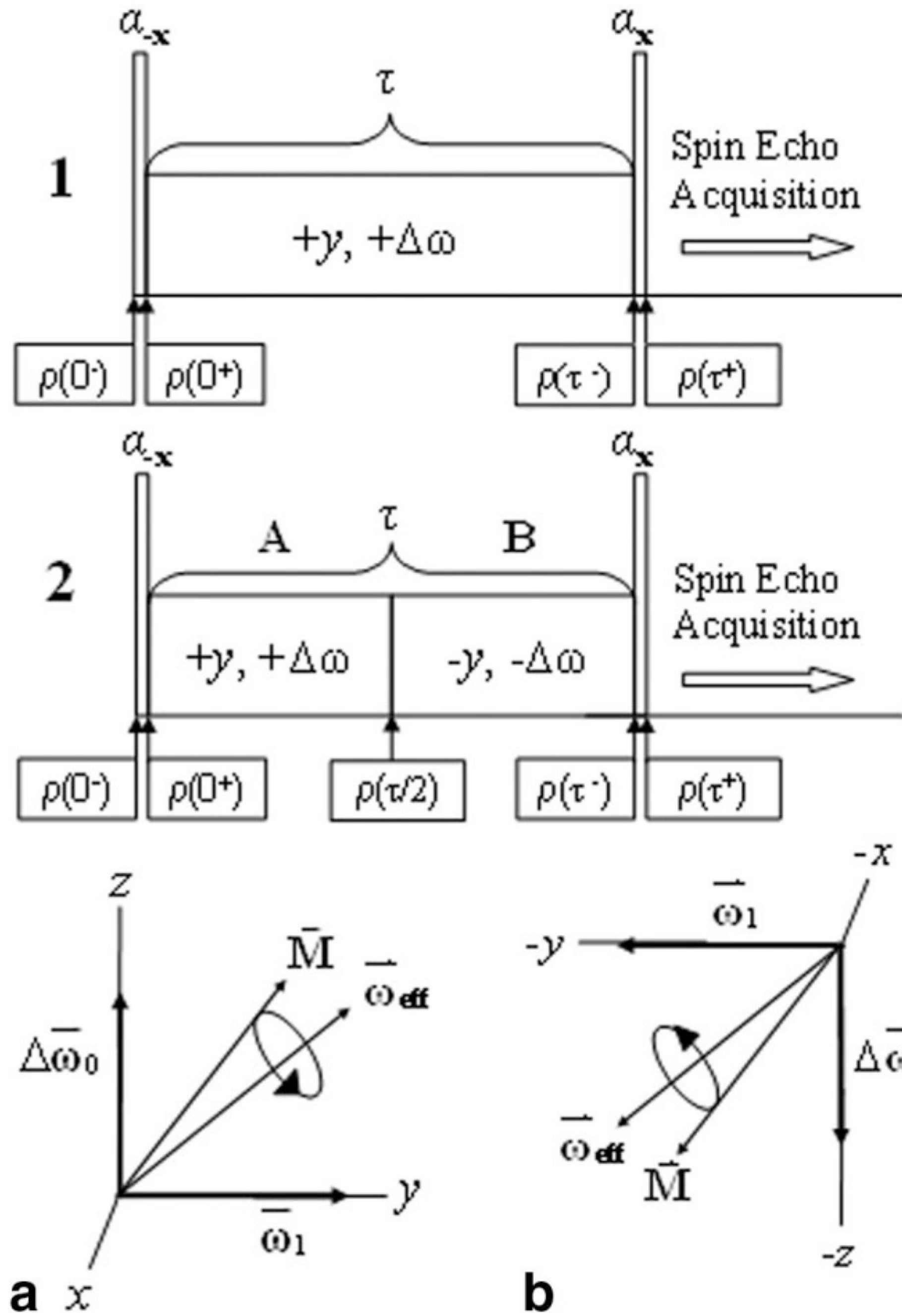

FIG. 2.

Two preparatory pulse clusters for $T_1\rho_{off}$-weighted imaging. **a**: In sequence 1, if the excitation flip angle α is not the same as that of the effective field **ϕ**, the magnetization nutates about ω_{eff} and produces imaging artifacts. **b**: In sequence 2, the magnetization is refocused by a frequency- and phase-inverted spin-locking pulse after τ/2.

NIH-PA Author Manuscript

NIH-PA Author Manuscript

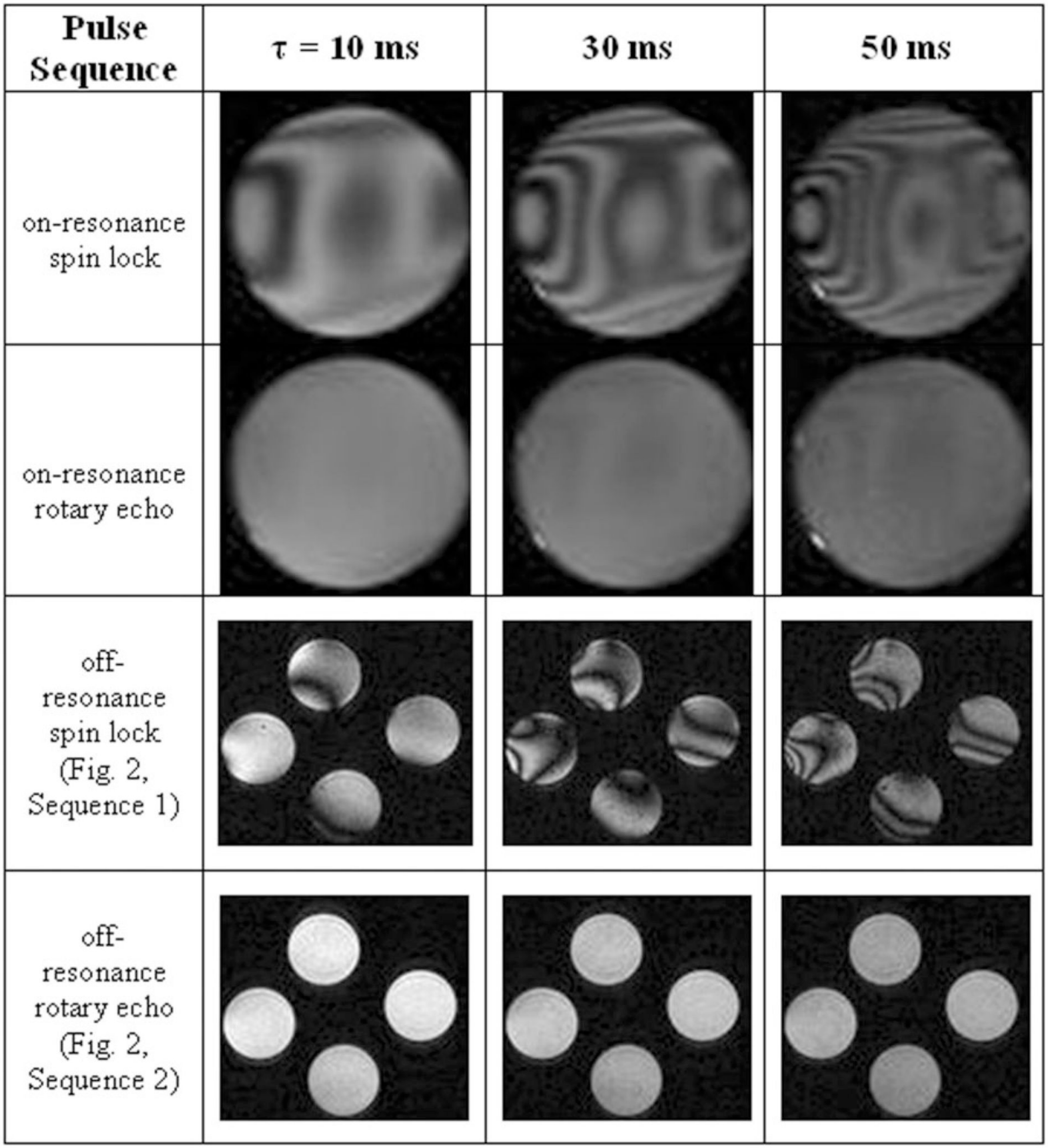

FIG. 3.

Compensation for B_1 inhomogeneity during on-resonance ($\Delta\omega_{RF} = 0$) and off-resonance ($\Delta\omega_{RF} = 400$ Hz) spin locking in 3% agarose phantoms ($\alpha = 65°$, $\omega_1 = 400$ Hz). Magnetization nutates about the effective field ω_{eff}, and without both phase and frequency inversion, banding artifacts are severe.

Pulse Sequence	Off-resonance spin lock (Fig. 2, Sequence 1)	Off-resonance rotary echo (Fig. 2, Sequence 2)
τ = 20 ms	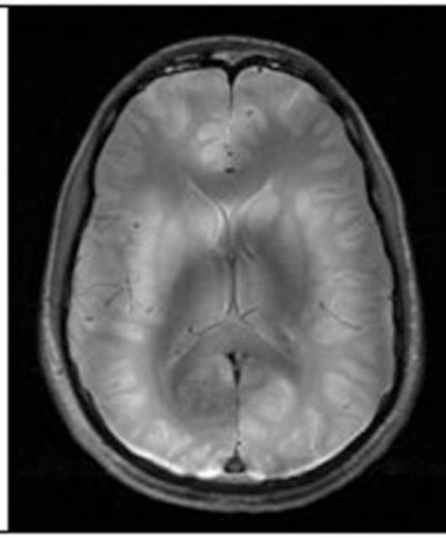	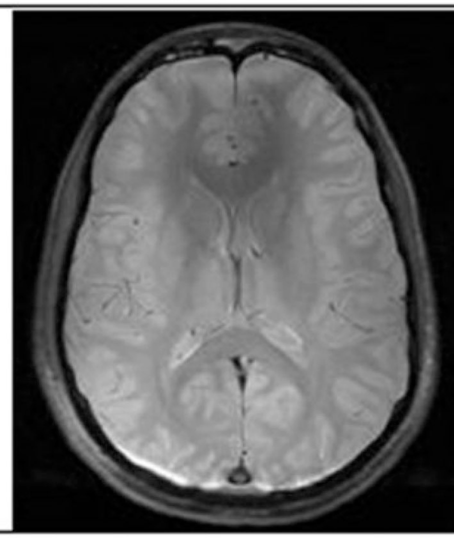

FIG. 4.
$T_1\rho_{off}$-weighted brain images obtained in a healthy volunteer at 3T (α = 65°, ω_1 = 400 Hz, $\Delta\omega_{RF}$ = 400 Hz). Phase and frequency alternation of the spin-lock pulse compensates for imperfect flip artifacts; however, there is signal loss in regions of $\Delta\omega_0$ inhomogeneity. The flip angle α = 65° deviates from the nominal $\tan^{-1}(\omega_1/\Delta\omega)$ = 45° flip necessary for an off-resonance spin lock, and was chosen to amplify the image artifacts.

Table 1

Sources of Artifacts in $T1\rho_{off}$-Weighted Imaging and Their Pulse Sequence Correction Schemes.

	Reference	B_1 imperfections (on-resonance)	B_1 imperfections (off-resonance)	Flip angle $\alpha \neq \varphi(\varphi = 90°$ on-resonance)
Conventional[a]				
Rotary echo	Wheaton et al. (8)	X		X
Adiabatic excitation	Santyr et al. (16)			X
Off-resonance rotary echo	This work	X	X	X

[a] A conventional spin-lock is an on-resonance spin lock without a rotary echo and is sensitive to all three sources of artifacts in $T1\rho$-weighted imaging.